

# Cannabinoid receptor activation in the juvenile rat brain results in rapid biomechanical alterations: Neurovascular mechanism as a putative confounding factor

Simon Chatelin<sup>1,4</sup>, Marie Humbert-Claude<sup>2,4</sup>,  
 Philippe Garteiser<sup>1</sup>, Ana Ricobaraza<sup>2</sup>, Valérie Vilgrain<sup>1,3</sup>,  
 Bernard E Van Beers<sup>1,3</sup>, Ralph Sinkus<sup>1,4</sup> and Zsolt Lenkei<sup>2,4</sup>

## Abstract

We have recently reported cannabinoid-induced rapid changes in the structure of individual neurons. In order to investigate the presence of similar effects at the regional level, measures of brain tissue biomechanics are required. However, cannabinoids are known to alter cerebral blood flow (CBF), putatively resulting in presently unexplored changes in cerebral tissue biomechanics. Here we used magnetic resonance elastography (MRE) and flow-sensitive alternating inversion recovery (FAIR) imaging to measure *in vivo* alterations of mechanical properties and CBF, respectively, in the rat hippocampus, a brain region with a high density of type-1 cannabinoid receptors (CB<sub>1</sub>R). Systemic injection of the cannabinoid agonist CP55,940 (0.7 mg/kg) induced a significant stiffness decrease of  $10.5 \pm 1.2\%$  at 15 minutes. FAIR imaging indicated a comparable decrease ( $11.3 \pm 1.9\%$ ) in CBF. Both effects were specific to CB<sub>1</sub>R activation, as shown by pretreatment with the CB<sub>1</sub>R-specific antagonist AM251. Strikingly, similar rapid parallel changes of brain elasticity and CBF were also observed after systemic treatment with the hypotensive drug nicardipine. Our results reveal important drug-induced parallel changes in CBF and brain mechanical characteristics, and show that blood flow-dependent tissue softening has to be considered as an important putative confounding factor when cerebral viscoelastic changes are investigated.

## Keywords

Cannabinoid receptors, cerebral blood flow, elasticity imaging, elastography, magnetic resonance imaging

Received 6 February 2015; Revised 16 June 2015; Accepted 3 August 2015

## Introduction

The type-1 cannabinoid receptor (CB<sub>1</sub>R) has initially been identified as the main neuronal target of  $\Delta^9$ -tetrahydrocannabinol ( $\Delta^9$ THC), the major psychoactive substance of marijuana. CB<sub>1</sub>Rs are widely distributed in neurons of the cerebral cortex, hippocampus, basal ganglia, amygdala and cerebellum and are the major mediators of endocannabinoid signalling in the brain. CB<sub>1</sub>Rs are mainly recognized as key players in the regulation of neurotransmission<sup>1</sup> but several lines of evidence suggest that CB<sub>1</sub>Rs also act as regulators of neuronal structure. Chronic CB<sub>1</sub>R activation induces structural alterations both *in vivo*<sup>2,3</sup> and *in vitro*<sup>4</sup> and

structural remodeling has also been observed at a short-time scale *in vitro*.<sup>5,6</sup> Notably, our recent report

<sup>1</sup>Laboratory of Imaging Biomarkers, UMR1149 INSERM-University Paris Diderot, Sorbonne Paris Cité, Paris, France

<sup>2</sup>Brain Plasticity Unit, CNRS UMR8249, ESPCI-ParisTech, PSL Research University, Paris, France

<sup>3</sup>Department of Radiology, Assistance-Publique Hôpitaux de Paris, Clichy, France

<sup>4</sup>These authors contributed equally to this work

## Corresponding author:

Zsolt Lenkei, Brain Plasticity Unit, ESPCI-ParisTech, CNRS UMR8249, F-75005 Paris, France.  
 Email: [zsolt.lenkei@espci.fr](mailto:zsolt.lenkei@espci.fr)

suggests that CB<sub>1</sub>R can rapidly transform the neuronal cytoskeleton through actomyosin contractility, resulting in cellular remodeling events ultimately able to affect brain architecture and wiring.<sup>7</sup> These data suggest that the activation of CB<sub>1</sub>R, one of the most highly expressed brain G protein-coupled receptors (GPCRs), might also result in rapid structural changes in the developing brain *in vivo*, although such an effect has not yet been demonstrated.

One of the reasons for this lack of knowledge is the technical difficulty involved in the detection of rapid changes in the structure and biomechanics of the living brain. In addition to the challenge of measuring the biomechanical parameters of living neuronal tissue, CB<sub>1</sub>R-induced changes in cerebral blood flow (CBF) might also represent a confounding factor. Notably, CB<sub>1</sub>R<sub>s</sub> are also expressed in micro-vascular endothelial cells<sup>8</sup> and in smooth muscle cells<sup>9</sup> of the cerebral vasculature, which play a major role in the mediation of vasodilatation.<sup>10</sup> To date, a link between the perfusion of the brain and its mechanical properties has only been demonstrated *in vitro*.<sup>11</sup> Recent *in vivo* studies provide strong evidence of biomechanical changes following perfusion fluctuations in organs such as the liver or kidney,<sup>12</sup> but similar rapid correlations between tissue biomechanics and perfusion have yet to be demonstrated in the living brain.

While mechanical properties of the young brain were previously measured either *ex vivo*<sup>13,14</sup> or invasively *in vivo*,<sup>15,16</sup> the presence of non-physiological blood perfusion and metabolic conditions resulted in highly different elasticity values hindering the establishment of consensus reference values. The CBF is also changing throughout the life. For instance, a 70% increase in the signal-to-noise ratio of the arterial spin labeling (ASL) perfusion MRI images and a 30% increase in the absolute cerebral blood flow compared to the adult data were observed.<sup>17</sup>

Magnetic resonance elastography (MRE) is a magnetic resonance imaging (MRI) technique capable of exploring the biomechanical properties of soft tissue *in vivo* by measuring cyclic displacements of propagating shear waves.<sup>18</sup> Increasing MRE-based evidence suggests that the mechanical properties of living soft tissue are sensitive markers of its structure, vasculature and perfusion, which can be influenced by a variety of biological factors, such as brain tumors,<sup>19</sup> multiple sclerosis<sup>20</sup> and neurodegenerative processes.<sup>21</sup> Pathological processes such as acute neuroinflammation have also been recently shown to cause reductions in the mechanical cohesion of brain tissue and subsequent reversible decreases in elasticity and viscosity.<sup>22</sup> Similarly, changes in the neural density after stroke have been shown *via* MRE to induce modifications in viscoelastic cerebral properties.<sup>23</sup> A recent study

demonstrated that brain mechanical properties measured by MRE are also markers of the modification of brain tissue micro-architecture, by showing a link between viscoelasticity and histologically detected cortical myelin content during an active demyelination protocol of the mouse *corpus callosum*.<sup>24</sup> Interestingly, in this study *corpus callosum* viscoelasticity showed rapid increase (~20% between weeks 3 and 9) until stabilization around nine weeks of age, showing that brain maturation is accompanied by measurable and significant changes in brain biomechanical parameters.

The objective of this study was to apply parallel *in vivo* measurements of CBF and mechanical brain characteristics to better understand their relation. To measure perfusion-induced bio-mechanical changes, CBF was measured by an MRI-based imaging technique, flow-sensitive alternating inversion recovery (FAIR) perfusion imaging, during systemic treatment with both a cannabinoid agonist and the hypotensive drug nicardipine. In parallel, we used MRE to identify local alterations of mechanical properties induced by systemic cannabinoid or nicardipine treatment, by focusing on the hippocampus, a cerebral structure with high CB<sub>1</sub>R-density in the juvenile rat brain.

## Material and methods

### Drug preparation

CP55,940 (synthetic cannabinoid receptor agonist) and AM251 (specific type-1 cannabinoid receptor antagonist) were obtained from Tocris (Bristol, UK). CP55,940 and AM251 were dissolved at final concentrations of 0.2 mg/ml and 0.9 mg/ml respectively, in vehicle. Vehicle solution was composed by 80% volume of 0.9% NaCl, 10% volume of DMSO and 10% volume of Tween 80 (Sigma Aldrich). Nicardipine, a dihydropyridine-type Ca<sup>2+</sup> channel blocker with high vascular selectivity and strong cerebral and coronary vasodilatory activity (Aguettant Laboratories, Lyon, France), was used undiluted, at 10 mg/ml.

### Drug application

All experiments were performed in agreement with the European Community Council Directive of 22nd September 2010 (010/63/UE) and the local ethics committee "Comité d'éthique en matière d'expérimentation animale n°59, C2EA – 59, 'Paris Centre et Sud'" (agreement #2014-14). The number of animals in our study was kept to the necessary minimum and we have followed the ARRIVE guidelines for the report of the experiments. The measurements were conducted on healthy randomized male or female Sprague-Dawley rats weighing 20–30 g and aged from 10 to 12 days

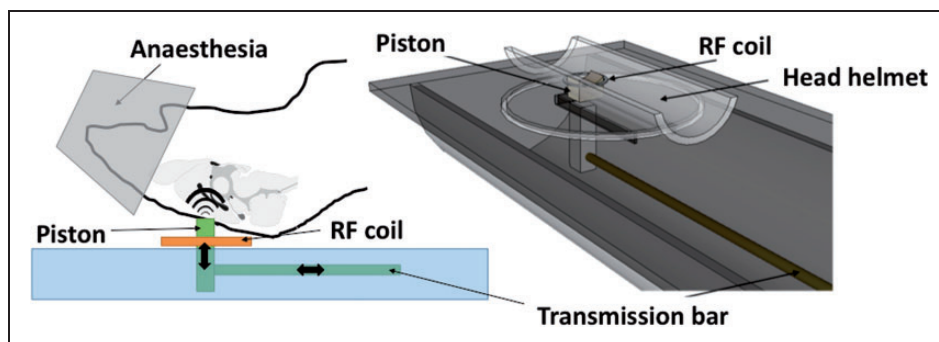


**Figure 1.** Schematic view of the MRE experimental setup. Seven Tesla small animal MRI scanner (Pharmascaan, Bruker BioSpin). A carbon fiber rod transmits vibrations from a remote vibration generator to a piston in contact to the head of the animal, which is maintained in supine position above the surface coil by an adapted head helmet. The entire setup is inserted within the volume transmit coil of the MR system.

(Janvier-Europe laboratories, Saint Berthevin, France). Sex-dependent differences were not investigated in this study. Rats were housed in a 12–12-h light-dark cycle room at 22°C. CP55,940 (0.7 mg/kg), AM251 (3 mg/kg), nicardipine (15 mg/kg) or vehicle (2 ml/kg) were injected intraperitoneally. Animals that died or moved during the acquisitions were excluded from the analysis (mortality rate: 12.8% and 5.9% for MRE and FAIR imaging, respectively). For MRE experiments, a total of 20 rats received CP55,940 injections, preceded by an injection of either the antagonist AM251 ( $n=6$  total, all successfully tested) or the vehicle ( $n=14$  total; 11 successfully tested, three excluded due to mortality). The control group was assessed by performing two repeated injections of vehicle ( $n=7$  total; five successfully performed, two excluded due to mortality). In order to confirm the absence of effect of AM251 injected alone, a second control group of rats underwent a pre-injection of AM251 followed by an injection of vehicle ( $n=3$  total, all successfully tested). To assess the effect of a brain vasodilatation on mechanical properties, a single injection of nicardipine was performed ( $n=9$  total; eight successfully tested, one excluded due to movement). In FAIR experiments, the CBF values were recorded in a total of 19 rats, after injection of either CP55,940 ( $n=8$  total; six successfully performed, two excluded due to mortality), nicardipine ( $n=8$  total; five successfully performed, one excluded due to mortality, two excluded due to movement) or AM251 + CP55,940 ( $n=3$  total, all successfully tested).

### MRI and MRE acquisitions

Cerebral MRI and MRE were performed on a 7-Tesla small animal MRI scanner (Pharmascaan, Bruker Biospin SA, Wissembourg, France). All experiments were performed on anesthetized rats, using 1–2% isoflurane in 50% O<sub>2</sub> and 50% air with a facemask

(Matrx<sup>TM</sup> VIP 3000, Midmark Corp., OH, USA). The respiration was monitored (Small Animal Instruments 1025L, Stony Brook, NY, USA). For the MRE acquisitions, mechanical waves were generated using a uni-axial modal exciter vibrating at 1000 Hz (Bruel & Kjaer 4808, Naerum, Denmark). The waves were transmitted from the exciter to a piston through a carbon fiber rod using a custom-made set-up (Figure 1). The piston was positioned against the top of the rat skull (supine position) which was embedded in a plaster helmet. The vibration of the piston induces the vibration of the skull and consequently of the brain. A volume coil was used for MRI excitation and a 20 mm diameter surface coil positioned below the top of the head was used for MRI signal acquisition. After standard calibration, piloting and shimming, high-resolution axial T2-weighted images were acquired with the following parameters: a Multi Slice Multi Echo sequence (MSME), a repetition time (TR) of 2000 ms, an echo time (TE) of 63 ms, a slice thickness of 1 mm, an acquisition matrix of 256 × 256, a field of view (FOV) of 30 mm, one average, on 10 slices, resulting in an acquisition time of 8 min. Afterwards, T2-weighted images centered on the hippocampus in an axial orientation were acquired with the following parameters: a MSME, a TE/TR of 63/2000 ms, a slice thickness of 0.3 mm, an acquisition matrix of 128 × 128, a FOV of 19.2 mm, one average, 10 slices, resulting in an acquisition time of 3 min. Then, the 3D-MRE scanning parameters included the following: a SE sequence with synchronous 1000 Hz motion-encoding gradients to encode three orthogonal displacement maps in phase images; a TE/TR of 19.5/901 ms, a slice thickness of 0.3 mm, an acquisition matrix of 64 × 64, a FOV of 19.2 mm, one average, 10 slices, resulting in an acquisition time of 7 min per direction, leading to 21 minutes on the three consecutive directions. A minimum of four time steps of the shear wave

were acquired for each image. This first MRE examination, considered as a baseline acquisition for each animal, was followed by the injections of drugs. Fifteen and 60 min after the injection, a second and a third MRE examination were, respectively, performed.

Shear mechanical properties were reconstructed from the acquired MRE data (small cyclic displacements) using published algorithms,<sup>25</sup> by an investigator blind to the treatment protocol. Results are presented in terms of absolute value  $|G^*| = (G'^2 + G''^2)^{1/2}$  of the complex shear modulus, of which real  $G'$  – storage modulus – and imaginary  $G''$  – loss modulus – parts correspond to the stored energy (elastic part) and the energy dissipated or lost due to scattering (viscous part), respectively, when subjected to external forces. The magnitude of the complex valued shear modulus corresponds to the measurement of the stiffness of the tissue. Regions of interest (ROIs) were defined on anatomical images and copied onto the maps of reconstructed mechanical parameters providing mean values and standard deviations. Signal-to-noise ratio (SNR) measurements on the shear wave displacement maps were performed to assess the reliability and sensitivity of this methodology.

### Cerebral blood flow map by flow sensitive alternating inversion recovery

Cerebral blood flow (CBF), a measurement of the blood perfusion in units of ml of blood/min/100 g of tissue, was quantified using a flow sensitive alternating inversion recovery (FAIR) sequence on the same small-animal 7-Tesla MR scanner. After standard calibration, piloting and shimming, first axial T2-weighted (MSME, TE/TR: 63/2 ms, 1 mm slice thickness; matrix 256 × 256, field of view (FOV) 3 cm, one average, 10 slices) images were acquired to localize the hippocampus. Cerebral perfusion maps were obtained by using the flow alternating inversion recovery technique (TE/TR: 19/4000 ms, 1 axial slice, 300 μm × 600 μm × 3 mm, five inversion times, 3 mm inversion slab thickness, interleaved mode). Briefly, images of longitudinal relaxation rates ( $R1 = 1/T1$ ) were calculated from the inversion recovery profiles obtained in the presence of the global (true  $R1$ ) or the selective (apparent  $R1'$ ) inversion pulses. The difference in  $R1$  between the two inversion modes was attributed to the perfusion of non-inverted spins in the labeled slice.<sup>26,27</sup> Cerebral perfusion ( $P$ , ml/(100 g × min)) was calculated as described by Kober et al. using the following relationship:  $P = \lambda \times (R1_{\text{blood}}/R1) \times (R1' - R1)$ , where  $\lambda$  is the blood tissue partition coefficient<sup>28</sup> (taken as 90 ml/g according to literature values<sup>29</sup>) and  $R1_{\text{blood}}$  is the relaxation rate of blood at 7 T (taken as 2400 ms,

according to the literature<sup>30</sup>). CBF was evaluated in manually drawn ROIs, positioned on the hippocampus, by an investigator blind to the treatment protocol. ROIs were defined on anatomical MR images and were copied onto the maps obtained by the FAIR acquisitions, providing mean values and standard deviations of the CBF. In each rat, four FAIR acquisitions were successively performed before injections, and provided reference values of CBF. After drug injection, FAIR acquisitions and CBF measurements were performed during 80 min, by performing one scan every seven minutes.

### Immunohistochemistry

The immunohistochemistry was performed on a single untreated control rat, deeply anesthetized with intraperitoneal pentobarbital injection (100 mg/kg) and perfused transcardially with 50 ml fixative solution containing 4% paraformaldehyde in 0.1 M phosphate buffer, pH 7.5. The brain was removed, post-fixed in 4% paraformaldehyde for 24 h at 4°C, cryoprotected in phosphate buffer and 20% sucrose, frozen in isopentane at -50°C and stored at -80°C until processing. The brain was sectioned with a cryostat (50 μm thick) at the same coronal orientation as MR images. After permeabilization during 30 min, incubation of Triton X-100 0.5% in 0.1 M PBS (Phosphate Buffered Saline), slices were blocked by 1 h incubation of 0.1% Triton X-100, 5% Normal Goat Serum (NGS) and 0.1 M PBS. Then, slices were incubated 24 h at 4°C with an anti- $CB_1R$  antibody directed at the C terminus of the  $CB_1$  receptor diluted 1:500 in the incubation solution (NGS: 0.5%, Triton X-100: 0.1%, PBS: 0.1 M, Azide: 0.1%).<sup>31</sup> After washing with PBS 0.1 M, sections were incubated for 2 h at room temperature, with an Alexa Fluor® 488 anti-rabbit IgG (1:200) (Invitrogen) diluted in the incubation solution. Images were taken on a Zeiss AxioImager M1 microscope (Carl Zeiss GmbH, Oberkochen, Germany), using a 20 × , 0.75 numerical aperture (NA) objective.

### Statistical analysis

Both  $|G^*|$  and perfusion values are expressed as mean ± SEM. Statistical analysis was performed using Statistica® software. For the MRE data, a paired *t*-test was used to compare elasticity measurements before and after injection. A two-way analysis of variance (ANOVA) followed by Newman Keul's post hoc test was used to assess the difference between treatments. The statistical analysis on the CBF measurements were performed using repeated-measures one-way ANOVA followed by a Bonferroni's multiple comparison *post-hoc* test.

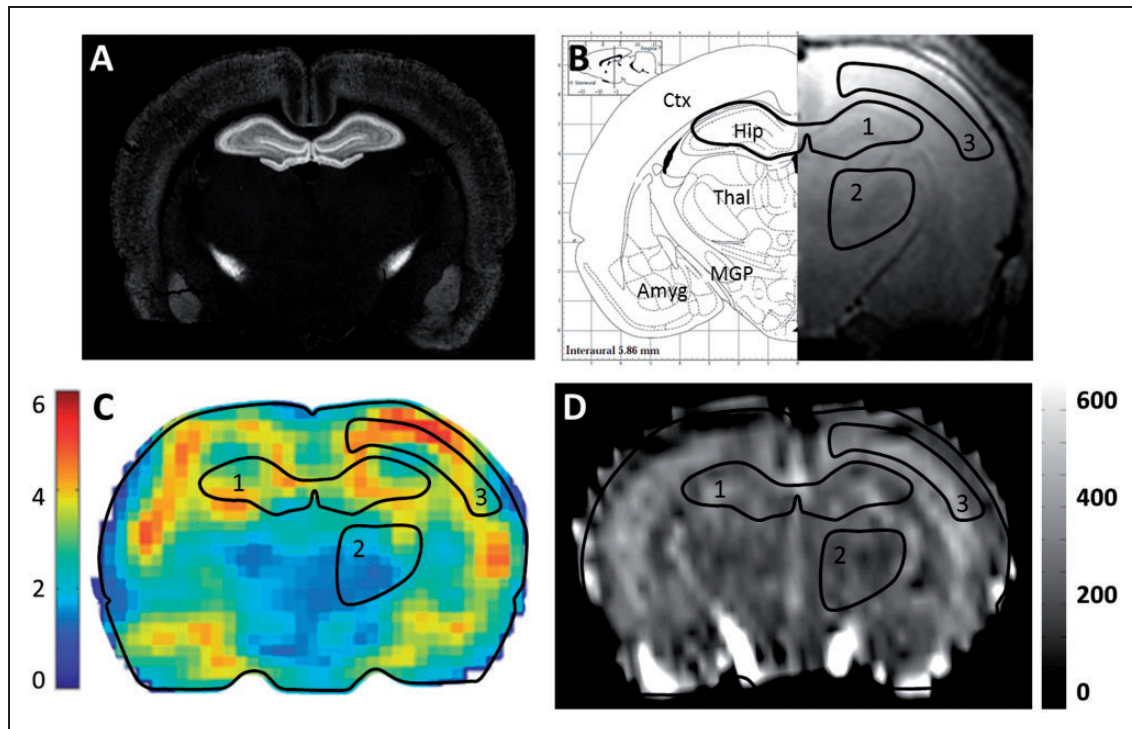


**Figure 2.** Parallel anatomical, MRI, MRE and CBF maps of a juvenile rat brain section. (a) CB<sub>1</sub>R immunolabeling on a coronal section of a rat brain at postnatal day 11. (b) Right: High-resolution coronal T2-weighted MRI image. Left: Corresponding brain atlas map from Paxinos G and Watson C, exhibiting three hand-drawn regions of interest used to extract mean values from both MRE and CBF maps (1: hippocampus, 2: thalamus, 3: cortical grey matter). Ctx: Cortex; Thal: Thalamus, Hip: Hippocampus; MGP: Medial Globus Pallidus, Amyg: Amygdala. (c) MRE map of the absolute values (kPa) of the complex-valued shear modulus  $|G^*|$ . (d) Cerebral blood flow map (ml/min/100 g).

## Results

### Localization of the CB<sub>1</sub>R in the juvenile rat brain

In order to select a region of interest (ROI) with high CB<sub>1</sub>R density, immunolabeling of the brain of a juvenile rat was performed. At the investigated forebrain level (Figure 2a and 2b), the purified anti-CB<sub>1</sub>R antibody produced moderate to strong labeling of the neocortex, the hippocampal formation, the pallido-nigral pathway of the basal ganglia and the basolateral complex of the amygdala. CB<sub>1</sub>R was poorly expressed in the *corpus callosum*, the thalamus and the hypothalamus. This distribution is coherent with previous reports, which, by using comparable experimental conditions in the adult brain, reported a high level of CB<sub>1</sub>R expression in a subset of GABAergic neurons in these regions.<sup>1,31</sup>

### Viscoelasticity and CBF maps of the juvenile rat brain

Three-dimensional (3D) displacement fields generated by the vibration source were acquired during the wave propagation in the brain (Supplementary Figure S1). From the MRE data, the absolute value of the complex valued shear modulus ( $|G^*|$ ) maps

were generated, as illustrated in Figure 2c. Analysis ROIs were defined from the high-resolution T2-weighted images, which allowed visualizing cerebral regions such as the hippocampus, the cerebral cortex and the thalamus (Figure 2b). Maps of the absolute values of the complex valued shear modulus provided mean reference viscoelasticity values in the hippocampus and thalamus of  $4.63 \pm 0.04$  kPa and  $3.60 \pm 0.07$  kPa, respectively ( $n = 33$  rats). The signal-to-noise ratio (SNR) was 1.7 times higher in the hippocampus (4.9) than in the thalamus (2.9). Due to reasons detailed in the Discussion section, MRE data were extracted only from the hippocampus ROI for further analysis (Table 1). To obtain CBF values, the same ROIs were applied (Figure 2d), yielding a reference CBF value of  $266.0 \pm 3.4$ ,  $253.8 \pm 17.7$  and  $233.4 \pm 5.0$  ml/min/100 g in the hippocampus, the thalamus and the cortex, respectively ( $n = 14$  rats).

### CB<sub>1</sub>R activation induces rapid softening of the hippocampus

MRE data are summarized in Table 1. The mean value of  $|G^*|$  measured in the hippocampus of 11 rats was  $4.91 \pm 0.18$  kPa at resting state (Figures 2c and 3a).

**Table 1.** Absolute values of the complex-valued dynamic shear modulus ( $|G^*|$ ) values measured in the hippocampus before and 15 min after injections.

Injection	MRE 1: Reference		MRE 2: injection + 15 min	
	$ G^* $ (kPa)	<i>n</i>	$ G^* $ (kPa)	<i>n</i>
CP55,940	4.91 ± 0.18	11	4.40 ± 0.19	11
AM251 +CP55,940	4.49 ± 0.22	6	4.39 ± 0.24	6
AM251	4.24 ± 0.16	3	4.11 ± 0.09	3
Vehicle	4.65 ± 0.17	5	4.48 ± 0.20	5
Nicardipine	4.47 ± 0.23	8	3.92 ± 0.25	8
Mean value	4.63 ± 0.04	33	–	33

Note: Data represent mean ± SEM and *n* the number of rats.

Fifteen minutes after the injection of the cannabinoid agonist CP55,940 (CP, 0.7 mg/kg), the  $|G^*|$  value decreased to  $4.40 \pm 0.19$  kPa, revealing a significant reduction of  $10.5 \pm 1.2$  % ( $P < 0.001$ ) (Figure 3a and 3b). This significant stiffness reduction was maintained at 60 min after injection (Figure 3b). In order to assess the involvement of CB<sub>1</sub>R in the CP effect, the CB<sub>1</sub>R-specific antagonist AM251 (3 mg/kg) was injected 15 min before CP. This AM251 pre-treatment completely inhibited the effect of CP (Figure 3c), demonstrating that the CP-induced softening of the hippocampus is due to CB<sub>1</sub>R activation. Neither the AM251 injected alone nor the vehicle solution had any effect on the elasticity of the hippocampus (Supplementary Figure S2).

In all treatment protocols, an absence of variation of the loss tangent  $\tan(\delta)$  was observed, with a mean value of  $0.15 \pm 0.002$ . Consequently, the capacity of the cerebral tissue to store energy (i.e. its elasticity) is systematically about 6.7 times higher than its capacity to lose energy (i.e. its viscosity), at the whole range of elasticity changes observed here. Therefore, the relative variations of the complex-valued shear modulus observed in this study are exactly the same for both the elastic  $G'$  and viscous  $G''$  modulus, indicating that both cerebral elasticity and viscosity show the same variation after drug injection.

### CB<sub>1</sub>R activation induces CBF decrease

The effect of CP55,940 on the CBF has been evaluated in six juvenile rats. Mean CBF values before CP55,940 injection were  $257.5 \pm 3.3$ ;  $247.7 \pm 2.1$  and  $226.4 \pm 2.8$  ml/min/100 g in the hippocampus, thalamus and cortex, respectively (Figure 2e). Fifteen minutes after CP55,940 injection, the CBF was  $228.3 \pm 4.1$ ,  $221.3 \pm 4.8$  and  $208.7 \pm 4.4$  ml/min/100 g, indicating a decrease of  $11.3 \pm 1.9$ %;  $10.7 \pm 2.0$ % and  $7.8 \pm 1.4$ %,

respectively ( $P < 0.001$ ) (Figure 3e). The CB<sub>1</sub>R antagonist AM251 injected at 15 min before the injection of CP55,940 completely inhibited this effect in all regions (Figure 3f), indicating that CP55,940-induced CBF decrease is specific to CB<sub>1</sub>R activation. These results suggest that cannabinoid-induced decrease of CBF may significantly contribute to cannabinoid-induced rapid changes in cerebral viscoelasticity.

### Assessment of the effect of a decreased CBF on the elasticity of the hippocampus

In order to directly investigate the effect of blood flow on cerebral viscoelasticity, we used the vasodilator drug nicardipine, a selective Ca<sup>2+</sup> channel blocker. The basal CBF evaluated in hippocampus of five rats was  $273.8 \pm 5.6$  ml/min/100 g. At 15 min following intraperitoneal injection of nicardipine at the dose of 15 mg/kg, the CBF decreased to  $229.8 \pm 8.3$  ml/min/100 g ( $P < 0.001$ ). This corresponds to a relative decrease of  $16.1 \pm 2.4$ % (Figure 3g), which is similar from those observed at 15 min after CP injections ( $11.3 \pm 1.9$ %).

In parallel, we measured  $|G^*|$  values at 15 min after nicardipine injection. The baseline  $|G^*|$  value was  $4.1 \pm 0.4$  kPa (Figure 3d). Importantly, at 15 min after nicardipine injection, the decrease of hippocampus stiffness was comparable to what was observed after CP injection, since it reached  $3.4 \pm 0.4$  kPa, corresponding to a change of  $12.7 \pm 5.3$ % ( $P < 0.001$ ) (Figure 3d).

These results suggest that changes in CBF and viscoelasticity are strongly correlated in the brain after injection of the vasodilator drug nicardipine.

## Discussion

As an important first step to establish the putative presence of rapid cannabinoid-induced biomechanical changes in the living brain, here we measured the effect of brain blood flow changes on brain tissue rigidity. Our results reveal important drug-induced parallel changes in cerebral blood flow and brain mechanical characteristics and show that perfusion-dependent tissue softening has to be considered when investigating changes in cerebral viscoelasticity.

### *In vivo* viscoelastic properties of the juvenile rat brain

Brain mechanical and functional properties are specific to the cerebral developmental stage. Mechanical properties of the juvenile brain are critical parameters in different medical domains, such as neurosurgery or traumatology. Here we present the first non-invasively obtained *in vivo* viscoelastic measurements of the juvenile rat brain. Shear mechanical properties indicated by

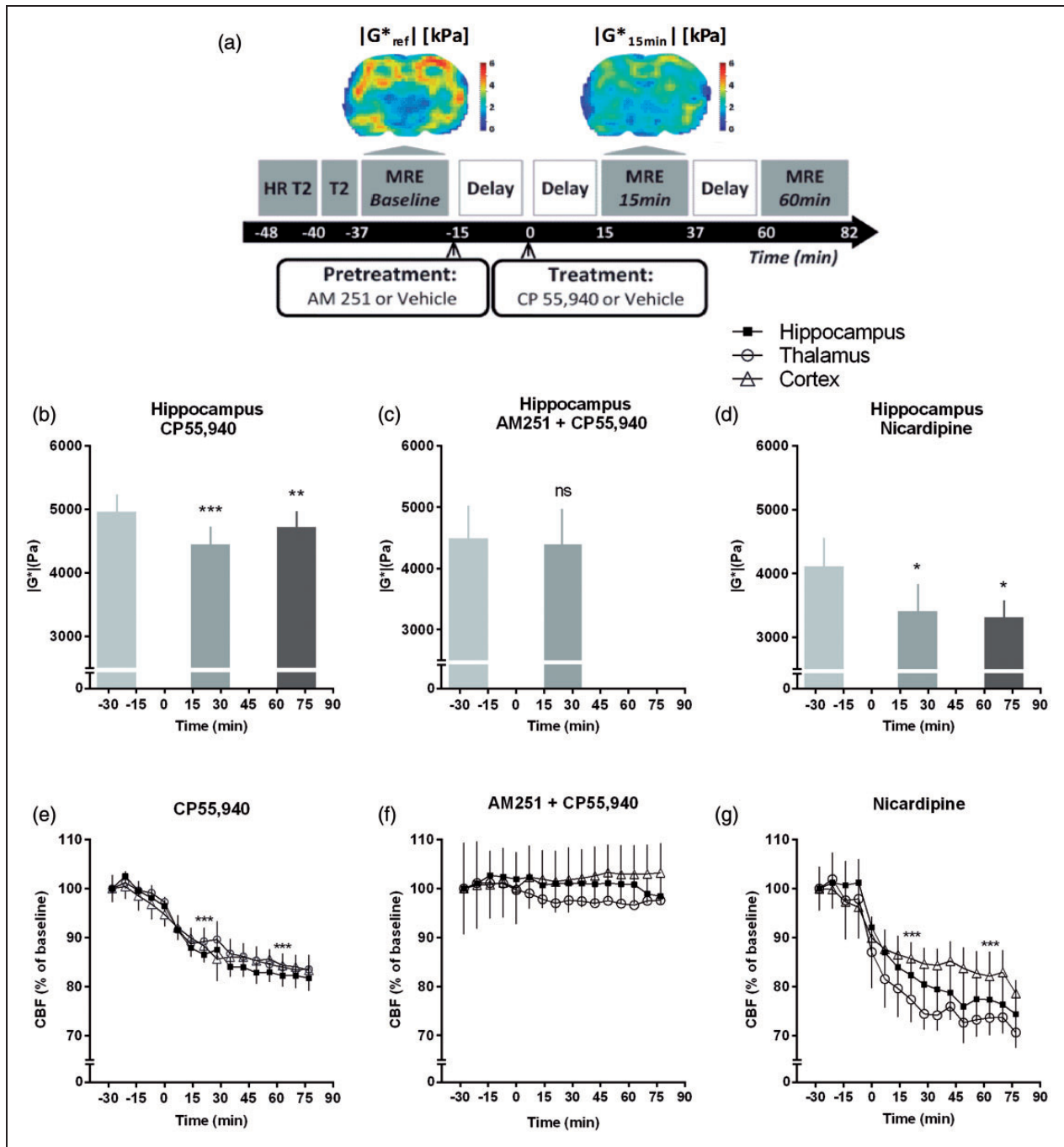


**Figure 3.** CB<sub>1</sub>R activation and nicardipine lead to a decrease of cerebral elasticity and blood flow. (a) Experimental protocol for MRI and MRE. A coronal section of the cerebral elasticity before and 15 minutes after CP55,940 (CP) injection is shown (Up). (b, c, d) Results are mean  $\pm$  SEM of the  $|G^*|$  quantified in the hippocampus. (b) CP55,940 injection induces a significant decrease of  $|G^*|$  at 15 min ( $10.5 \pm 1.2\%$ ,  $n = 11$ ) and 60 min ( $4.8 \pm 1.0\%$ ,  $n = 6$ ) after the injection. (c) The AM251 (3 mg/kg, i.p.), injected 15 min before CP (0.7 mg/kg, i.p.), inhibits the effect of the CP ( $n = 6$ ). (d) Nicardipine (15 mg/kg, i.p.) induces a significant decrease of the  $|G^*|$  at 15 min ( $12.7 \pm 1.9\%$ ,  $n = 8$ ) and 60 min ( $18.9 \pm 3.8\%$ ,  $n = 3$ ) after the injection. Statistical analysis: \* $P < 0.05$ , \*\* $P < 0.01$ , \*\*\* $P < 0.001$  versus baseline. Paired  $t$ -test (for C) or repeated measures one-way ANOVA following by a Bonferroni's multiple comparison *post-hoc* test. (e, f, g) Results are mean  $\pm$  SEM of the CBF expressed as percentage of the baseline which represents  $257.5 \pm 3.3$ ;  $247.7 \pm 2.1$  and  $226.4 \pm 2.8$  ml/min/100 g in the hippocampus, the thalamus and the cortex, respectively. (e) The CB<sub>1</sub>R agonist CP (0.7 mg/kg, i.p.) induces a significant decrease of the CBF in all the regions analyzed (\*\*\*\* $P < 0.001$ ,  $n = 6$ ). (f) The selective CB<sub>1</sub>R antagonist AM251 (3 mg/kg, i.p.), injected 15 minutes before CP (0.7 mg/kg, i.p.) inhibits the effect of the CP ( $n = 3$ ). (g). Nicardipine (15 mg/kg, i.p.) induces a significant decrease of the CBF in all the regions analyzed (\*\*\*\* $P < 0.001$ ,  $n = 5$ ).

$|G^*|$  values are significantly higher in the hippocampus ( $4.91 \pm 0.61$  kPa) than in the thalamus ( $3.60 \pm 0.42$  kPa) ( $n = 11$  rats). Despite the lack of sensitivity of the measurement in some of these regions, the heterogeneity of the cerebral elasticity is in accordance with previous studies on adult<sup>32</sup> and juvenile brains.<sup>13–16</sup> The higher apparent rigidity of the hippocampus as compared to the thalamus could be due to the more organized layered structure of the hippocampus. Interestingly, comparable difference of stiffness between gray and the more organized white matter was observed *in vivo* in 25 healthy adult human brains.<sup>33</sup>

Taken together, MRE of juvenile rat brain is a valid tool to measure changes of juvenile rat brain mechanical properties.

### *The relationship between brain viscoelastic properties and CBF*

In the present study, *in vivo* MRE coupled to FAIR measurements allowed investigation of parallel changes in hippocampus elasticity and blood flow on a short time scale. While *in vivo* data has been recently obtained by linking ischemia and decrease of cerebral elasticity in the rat brain after stroke, the potential confounding effects of tissue necrosis did not allow a definitive conclusion on the relationship between brain viscoelastic properties and CBF<sup>34</sup> to be made. Here, we observed that nicardipine, a selective blocker of L-type voltage-gated  $Ca^{2+}$  channels in the smooth muscle of cerebral and coronary blood vessels, induced a parallel decrease of CBF and brain elasticity. This result is in accordance with *in vitro* studies on the brain<sup>11</sup> and with *in vivo* studies performed in other organs such as the liver or kidney.<sup>12</sup> Previous studies showed an impact of age on brain viscoelasticity that has been attributed to modifications of brain structure.<sup>16,21</sup> However, a significant decline of CBF with advancing age has been showed by Chen et al.<sup>35</sup> By linking cerebral blood flow to mechanical properties, our study suggests that potential changes in CBF may also contribute to the above reported age-related modifications of brain mechanical properties.

To conclude, our findings show that the CBF must be taken into account in the interpretation of cerebral MRE-provided data.

### *The softening of the hippocampus induced by the $CB_1R$ activation*

The dorsal hippocampus, by expressing a high density of  $CB_1Rs$ , and by being close to the surface coil, is in optimal position for the measurement of putative cannabinoid-induced mechanical changes by MRE. Indeed, we were able to obtain adequately high SNR

to reliably measure changes in mechanical properties of this brain region.

Our study shows that i.p. injection of the cannabinoid receptor agonist CP55,940 (CP) at a dose of 0.7 mg/kg induces a  $10.5 \pm 1.2\%$  decrease of stiffness in the hippocampus at 15 min after injection. While CP55,940 targets both cannabinoid receptor subtypes ( $CB_1R$  as well as  $CB_2R$ ), the antagonist AM251 is selective for  $CB_1Rs$ . Consequently, AM251 pre-treatment confirmed that CP-induced rapid mechanical effects observed in this study are specific to  $CB_1Rs$ . To the best of our knowledge, similar acute effect of a drug on *in vivo* cerebral mechanical properties has not been reported yet. Importantly, parallel FAIR measurements showed that CP injection also induces a decrease of cerebral perfusion with similar amplitude ( $11.3 \pm 1.9\%$ ), which was inhibited by AM251 pre-treatment, showing that this effect is also  $CB_1R$ -specific. This result is in agreement with previously reported decrease of CBF in the rat hippocampus in response to  $\Delta^9THC$ .<sup>36</sup>  $CB_1Rs$  are highly expressed in endothelial cells<sup>8</sup> as well as cerebrovascular smooth muscle cells<sup>9</sup> and several mechanisms have been proposed to explain  $CB_1R$ -induced CBF decrease.<sup>37,38</sup> Interestingly,  $CB_1R$  agonists stimulate production of nitric-oxide (NO), a potent vasoactive molecule that induces CBF decrease. NO appears to be produced in response to  $CB_1$  receptor stimulation in a  $G_{i/o}$ -selective manner without an obvious  $Ca^{2+}$  transient.<sup>39</sup> Importantly, similarly to nicardipine treatment, the cannabinoid-induced changes in cerebral perfusion and  $|G^*|$  values are correlated, suggesting that the apparent rapid softening of the hippocampus after CP injection mainly results from perfusion decrease.

### *Limitations and perspectives*

The deeper laying thalamus presents relatively poor SNR compared to the hippocampus, which is explained by the important distance from the surface coil as well as from the vibrating piston, hindering precise measurement of elasticity changes in this structure. In addition, the cerebral cortex, which also expresses  $CB_1Rs$ , is adjacent to the skull, and potential artifacts caused by partial volume effects due to insufficient spatial resolution are likely. Indeed, close proximity with an extremely stiff object, such as the skull may generate artifacts in the wave inversion algorithms, affecting the reliability of the mechanical measurements in the cortical ROI. Consequently, in the present study, we focused on the dynamic measurements of brain mechanical properties only to the dorsal hippocampus ROI.

Previous studies have reported that perfusion is markedly increased in rats anesthetized with isoflurane

compared to perfusion in rats anesthetized with other anesthetic agents.<sup>40</sup> However, in our control tests (MRE as well as FAIR imaging), isoflurane animals (anesthetized using) were injected with the vehicle only. The stability of MRE (Figure S2) as well as FAIR values (data not shown) in these control conditions indicates that the duration of the anesthesia did not induce any significant variation of CBF or elasticity of the hippocampus over the time-course of the experiment. Finally, we used two controls, vehicle treatment and antagonist pre-treatment, to show that the effects of CP55,945 are specifically mediated by the CB<sub>1</sub> cannabinoid receptor.

The calculations of cerebral blood flow values were performed under the assumption of a constant value for  $\lambda$  the partition coefficient. This constant is derived from average tissue and blood water content according to literature values. This assumption is commonly accepted in FAIR perfusion studies. Whether the partition coefficient may in fact vary in response to the stimuli used in the present study remains to be examined. However, the range of potential variation of  $\lambda$  is strictly limited to the range between the value of brain (0.90) and at the most extreme possible case, the density of blood, which would amount to a partition coefficient of 1/1.06, or 0.94 ml blood/g tissue. This potential range of 4% for the variation of  $\lambda$  was considered to be sufficiently low to validate the hypothesis of a constant partition coefficient.

A current limitation of the study is the relatively long duration of MRE acquisition, thus protocols using shorter acquisition times will be necessary to identify effects occurring at time-scales shorter than 15 min. Especially, the measurement of both mechanical and perfusion properties is not triggered on the cardiac cycle inducing an averaging over cerebral blood pulsations. Finally, the lack of significant change of the loss tangent could be interpreted as either a conservation of the ratio between elasticity and viscosity after drug injection or a lack of sensitivity of the method to depict viscosity modifications. To our knowledge, no precedent from the literature describes *in vivo* modifications of the cerebral loss tangent with drug injection or blood flow modification.

## Conclusions

The present work shows that MRE is a useful tool to measure drug-induced viscoelastic changes in the living brain, however for agonism of CB<sub>1</sub> by CP55,940 the observed viscoelastic changes appear to be dominated by neurovascular causes. First, we show that MRE is able to produce heterogeneous maps of elasticity and viscosity of juvenile rat brains. Second, a correlation between cerebral perfusion and brain elasticity is

demonstrated, indicating that the CBF must be considered in the interpretation of cerebral MRE studies. Indeed, when blood pressure is changing, vascular pressure probably immediately affects vascular turgor and therefore cerebral mechanical properties. In this study, a significant temporal alteration of young rat hippocampus stiffness has been observed in a short delay after systemic cannabinoid injection, in correlation with a decrease of local cerebral blood flow. The use of combined MRE/FAIR techniques provides valuable information and opens new possibilities to investigate the drug-induced changes in cerebral biomechanics *in vivo*, as a complement to classical methods.

## Funding

The author(s) disclosed receipt of the following financial support for the research, authorship, and/or publication of this article: This work was supported by a grant to Z Lenkei and R Sinkus from the French Agence Nationale de la Recherche (ANR-09-MNPS-004-01). A Ricobaraza was supported by a postdoctoral fellowship from the Basque Country Government.

## Declaration of conflicting interests

The author(s) declared no potential conflicts of interest with respect to the research, authorship, and/or publication of this article.

## Authors' contributions

ZL, MH-C and SC designed the experiments; SC, MH-C, PG and AR performed the experiments; SC, PG, MH-C and RS analyzed the data; VV and BEVB supplied material support, SC, MH-C and ZL wrote the paper.

## Supplementary material

Supplementary material for this paper can be found at <http://jcbfm.sagepub.com/content/by/supplemental-data>

## References

1. Freund TF, Katona I and Piomelli D. Role of endogenous cannabinoids in synaptic signaling. *Physiol Rev* 2003; 83: 1017–1066.
2. Lawston J, Borella A, Robinson JK, et al. Changes in hippocampal morphology following chronic treatment with the synthetic cannabinoid WIN 55,212-2. *Brain Res* 2000; 877: 407–410.
3. Tagliaferro P, Javier Ramos A, Onaivi ES, et al. Neuronal cytoskeleton and synaptic densities are altered after a chronic treatment with the cannabinoid receptor agonist WIN 55,212-2. *Brain Res* 2006; 1085: 163–176.
4. Vitalis T, Laine J, Simon A, et al. The type 1 cannabinoid receptor is highly expressed in embryonic cortical projection neurons and negatively regulates neurite growth *in vitro*. *Eur J Neurosci* 2008; 28: 1705–1718.

5. Ishii I and Chun J. Anandamide-induced neuroblastoma cell rounding via the CB1 cannabinoid receptors. *Neuroreport* 2002; 13: 593–596.
6. Berghuis P, Rajniecek AM, Morozov YM, et al. Hardwiring the brain: endocannabinoids shape neuronal connectivity. *Science* 2007; 316: 1212–1216.
7. Roland AB, Ricobaraza A, Carrel D, et al. Cannabinoid-induced actomyosin contractility shapes neuronal morphology and growth. *eLife* 2014; 3: e03159.
8. Chen Y, McCarron RM, Ohara Y, et al. Human brain capillary endothelium: 2-arachidonoglycerol (endocannabinoid) interacts with endothelin-1. *Circulation Res* 2000; 87: 323–327.
9. Gebremedhin D, Lange AR, Campbell WB, et al. Cannabinoid CB1 receptor of cat cerebral arterial muscle functions to inhibit L-type  $Ca^{2+}$  channel current. *Am J Physiol* 1999; 276: H2085–H2093.
10. Wagner JA, Jarai Z, Batkai S, et al. Hemodynamic effects of cannabinoids: coronary and cerebral vasodilation mediated by cannabinoid CB(1) receptors. *Eur J Pharmacol* 2001; 423: 203–210.
11. Guillaume A, Osmont D, Gaffie D, et al. Effects of perfusion on the mechanical behavior of the brain-exposed to hypergravity. *J Biomech* 1997; 30: 383–389.
12. Yin M, Chen J, Glaser KJ, et al. Abdominal magnetic resonance elastography. *Topics in Magnetic Resonance Imaging: TMRI* 2009; 20: 79–87.
13. Prange MT and Margulies SS. Regional, directional, and age-dependent properties of the brain undergoing large deformation. *J Biomech Eng* 2002; 124: 244–252.
14. Chatelin S, Vappou J, Roth S, et al. Towards child versus adult brain mechanical properties. *J Mech Behav Biomed Mater* 2012; 6: 166–173.
15. Gefen A, Gefen N, Zhu Q, et al. Age-dependent changes in material properties of the brain and braincase of the rat. *J Neurotrauma* 2003; 20: 1163–1177.
16. Shulyakov AV, Cenkowski SS, Buist RJ, et al. Age-dependence of intracranial viscoelastic properties in living rats. *J Mech Behav Biomed Mater* 2011; 4: 484–497.
17. Wang J, Licht DJ, Jahng GH, et al. Pediatric perfusion imaging using pulsed arterial spin labeling. *J Magnet Reson Imag* 2003; 18: 404–413.
18. Muthupillai R, Lomas DJ, Rossman PJ, et al. Magnetic resonance elastography by direct visualization of propagating acoustic strain waves. *Science* 1995; 269: 1854–1857.
19. Xu L, Lin Y, Han JC, et al. Magnetic resonance elastography of brain tumors: preliminary results. *Acta Radiol* 2007; 48: 327–330.
20. Wuerfel J, Paul F, Beierbach B, et al. MR-elastography reveals degradation of tissue integrity in multiple sclerosis. *NeuroImage* 2010; 49: 2520–2525.
21. Sack I, Beierbach B, Wuerfel J, et al. The impact of aging and gender on brain viscoelasticity. *NeuroImage* 2009; 46: 652–657.
22. Riek K, Millward JM, Hamann I, et al. Magnetic resonance elastography reveals altered brain viscoelasticity in experimental autoimmune encephalomyelitis. *NeuroImage Clin* 2012; 1: 81–90.
23. Freimann FB, Muller S, Streitberger KJ, et al. MR elastography in a murine stroke model reveals correlation of macroscopic viscoelastic properties of the brain with neuronal density. *NMR Biomed* 2013; 26: 1534–1539.
24. Schregel K, Wuerfel E, Garteiser P, et al. Demyelination reduces brain parenchymal stiffness quantified *in vivo* by magnetic resonance elastography. *Proc Natl Acad Sci U S A* 2012; 109: 6650–6655.
25. Sinkus R, Tanter M, Xydeas T, et al. Viscoelastic shear properties of *in vivo* breast lesions measured by MR elastography. *Magnet Reson Imag* 2005; 23: 159–165.
26. Kim SG, Tsekos NV and Ashe J. Multi-slice perfusion-based functional MRI using the FAIR technique: comparison of CBF and BOLD effects. *NMR Biomed* 1997; 10: 191–196.
27. Gardener AG, Gowland PA and Francis ST. Implementation of quantitative perfusion imaging using pulsed arterial spin labeling at ultra-high field. *Magnet Reson Med* 2009; 61: 874–882.
28. Kober F, Iltis I, Izquierdo M, et al. High-resolution myocardial perfusion mapping in small animals *in vivo* by spin-labeling gradient-echo imaging. *Magnet Reson Med* 2004; 51: 62–67.
29. Herscovitch P and Raichle ME. What is the correct value for the brain–blood partition coefficient for water? *J Cerebral Blood Flow Metab: Official Journal of the International Society of Cerebral Blood Flow and Metabolism* 1985; 5: 65–69.
30. Rane SD and Gore JC. Measurement of T1 of human arterial and venous blood at 7T. *Magnet Reson Imag* 2013; 31: 477–479.
31. Thibault K, Carrel D, Bonnard D, et al. Activation-dependent subcellular distribution patterns of CB1 cannabinoid receptors in the rat forebrain. *Cerebral Cortex* 2013; 23: 2581–2591.
32. Chatelin S, Constantinesco A and Willinger R. Fifty years of brain tissue mechanical testing: from *in vitro* to *in vivo* investigations. *Biorheology* 2010; 47: 255–276.
33. Kruse SA, Rose GH, Glaser KJ, et al. Magnetic resonance elastography of the brain. *NeuroImage* 2008; 39: 231–237.
34. Martin A, Mace E, Boisgard R, et al. Imaging of perfusion, angiogenesis, and tissue elasticity after stroke. *J Cerebral Blood Flow Metab: Official Journal of the International Society of Cerebral Blood Flow and Metabolism* 2012; 32: 1496–1507.
35. Chen JJ, Rosas HD and Salat DH. Age-associated reductions in cerebral blood flow are independent from regional atrophy. *NeuroImage* 2011; 55: 468–478.
36. Bloom AS, Tershner S, Fuller SA, et al. Cannabinoid-induced alterations in regional cerebral blood flow in the rat. *Pharmacol Biochem Behav* 1997; 57: 625–631.
37. Randall MD, Harris D, Kendall DA, et al. Cardiovascular effects of cannabinoids. *Pharmacol Therapeut* 2002; 95: 191–202.

38. Hillard CJ. Endocannabinoids and vascular function. *J Pharmacol Experiment Therapeut* 2000; 294: 27–32.
39. Carney ST, Lloyd ML, MacKinnon SE, et al. Cannabinoid regulation of nitric oxide synthase I (nNOS) in neuronal cells. *J Neuroimmune Pharmacol: The Official Journal of the Society on NeuroImmune Pharmacology* 2009; 4: 338–349.
40. Hendrich KS, Kochanek PM, Melick JA, et al. Cerebral perfusion during anesthesia with fentanyl, isoflurane, or pentobarbital in normal rats studied by arterial spin-labeled MRI. *Magnet Reson Med* 2001; 46: 202–206.